ResearchGate

See discussions, stats, and author profiles for this publication at: https://www.researchgate.net/publication/377474053

# A white laser resonator with chirped photonic crystals

**Article** *in* Optical Materials · January 2024

DOI: 10.1016/j.optmat.2024.114839

CITATIONS
0

READS
51

**3 authors**, including:

Ashot Gevorgyan
Yerevan State University
**286** PUBLICATIONS **1,611** CITATIONS
SEE PROFILE

Ilya Efimov Mikhailovich
Far Eastern Federal University
**26** PUBLICATIONS **51** CITATIONS
SEE PROFILE

All content following this page was uploaded by Ashot Gevorgyan on 18 January 2024.

The user has requested enhancement of the downloaded file.

Optical Materials xxx (xxxx) 114839

Contents lists available at ScienceDirect

Optical Materials

journal homepage: www.elsevier.com/locate/optmat

Research Article

# A white laser resonator with chirped photonic crystals

A.H. Gevorgyan *, N.A. Vanyushkin, I.M. Efimov

*Institute of High Technologies and Advanced Materials, Far Eastern Federal University, 10 Ajax Bay, Russky Island, 690922, Vladivostok, Russia*

ARTICLE INFO

*Keywords:*
White laser
Chirped photonic crystals
Chirping constant
Laser threshold
Density of states
Light localization

ABSTRACT

We investigate theoretically the possibilities of simultaneous laser generation in all, closely spaced modes of chirped photonic crystals layer in all visible region of the spectrum both for chirped rugate and chirped stratified photonic crystals. The spectra of reflection, field localization as well as relative photonic density of states and absorption for both rugate and stratified photonic crystals with different chirping parameters, as well as for a Fabry-Perot resonator are computed and compared. It was shown that there are two kinds of modes in chirped photonic crystals: edge modes and bound modes. We also calculated the threshold values for mentioned structures. In addition, we note that with the ability to control the chirp contrast, it becomes possible to obtain a white laser with a simple system on a chip, which can find wide application ranging from miniaturized coherent light source, optical sensing, to visible light communication.

## 1. Introduction

Although lasers were invented in the 60s of the last century interest in them does not decrease, and even, on the contrary, increases year by year. They have become an integral part of our lives, they are present everywhere, at home, in medicine, in science, in industry, etc.

It must be noted that early theories of laser resonators established that even simple resonators can produce complex spatially structured modes. Initially, researchers focused on distinguishing and selecting individual modes to create well-defined single modes [1]. Increasingly, however, emerging applications require going beyond single modes to create complex light patterns, sometimes referred to as structured light. Structured light refers to the tailoring or shaping of light in all its degrees of freedom whether in time and frequency, to create ultrafast tailored time pulses; or, more commonly, mainly, in controlling light's spatial transverse degrees of freedom such as polarization, amplitude and phase [2]. Structured light found application in optical trapping and tweezing, in super-resolution microscopy, in manufacturing, in optical communications and security, in imaging, and laser-based computational solvers [1,2].

Not only is spatially structured light of interest, but also the simultaneous generation of frequency structured modes in a laser resonator. In particular, multi-color (multi-wavelength) lasers over the full visible color spectrum from a single chip device have been a subject of great interest in recent years [3–9]. Their ultimate forms are the white lasers [7–14], the high directionality, brightness, and capability to modulate the intensity which are highly important, allowing enhancement of the signal-to-noise ratio in spectroscopic systems, the sensitivity of detection devices, data transmission rates, and the color rendering in lighting elements. White lasers can find applications in modern science and techniques, in laser lighting, in full-color laser imaging and display, in biological and chemical sensing, scanning, and monitoring, in ultra-fast data transfer, in spectroscopy, as miniaturized coherent light source [15–30]. According to the chromatic diagram, the simultaneous emission of red, green, and blue (RGB) colors can form white lasers, and furthermore, to adjust the chromaticity or improve the color rendering quality, yellow must be added to form the simultaneous emission of red, yellow, green, and blue (RYGB) colors, which can also create a white laser [10–12]. The design of such laser devices is challenging due to the material requirements for producing multi-color output and the complex design for generating laser action, to the balance performance for wide bandwidth, to the high average and peak power, to the high pulse energy, to the high spatial and temporal coherence, and to the profile-driven spectrum. And work in this direction is intensively continuing. Thus, the creation of simple, easy to manufacture, easily controllable systems on a chip with the possibility of simultaneous laser generation on many modes in the visible region of the spectrum is very relevant. Recently, studies of the possibilities of multi-wave laser generation in disordered systems, and especially white random lasers have been of great interest, too [31,32].

On the other hand, for multimode laser generation in a wide frequency region, and on many modes one can use a chirped, distributed

* Corresponding author.
*E-mail addresses:* agevorgyan@ysu.am (A.H. Gevorgyan), vaniuschkin.nick@ya.ru (N.A. Vanyushkin), efimov.im@dvfu.ru (I.M. Efimov).

https://doi.org/10.1016/j.optmat.2024.114839
Received 3 October 2023; Received in revised form 1 January 2024; Accepted 2 January 2024
0925-3467/© 20XX

CORRECTED PROOF

Note: Low-resolution images were used to create this PDF. The original images will be used in the final composition.

Bragg reflector (DBR) photonic crystal (PC) structure. In chirped PCs (PCs with a gradient of unit cell size) essential broadening of photonic band gap (PBG) takes place [33–35]. In chirped PCs a strong wavelength-dependent localization of electromagnetic wave inside the PC at its spatial positions (rainbow trapping) takes place [36–43], too. In the review article [44], the optical properties of 1D periodic, aperiodic and disordered structures are discussed, some theoretical methods for studying the structures are described, and the refractive indices of the most used materials, optical response, fabrication methods and some of the most important applications of 1D structures such as sensing, light amplification and light capture for photovoltaic devices, different types of disorder in 1D photonic structures are considered. In Ref. [45] the features of the light localization, absorption, light energy density and photonic density of states in 1D chirped rugate (with continuous change of the refractive index) PCs were investigated.

In this paper we will theoretically investigate the possibilities of simultaneous multiwavelength laser generation by chirped PCs at different values of contrast of chirping both in chirped rugate and stratified PCs.

## 2. Results and discussion

Firstly, we, as in Ref. [45], will consider a chirped rugate 1D PC of the form (Fig. 1(a))

$$\varepsilon(z) = \varepsilon + \Delta\varepsilon \sin\left(\frac{2\pi}{\Lambda(z)} z\right) \tag{1}$$

where $\epsilon$ is the constant value, $\Delta\varepsilon$ and $\Lambda(z)$ are the depth and the period of modulation, correspondingly. The PC layer with thickness $L$ is sandwiched between the planes $z = 0$ and $z = L$, and $\varepsilon_s = 1$, where

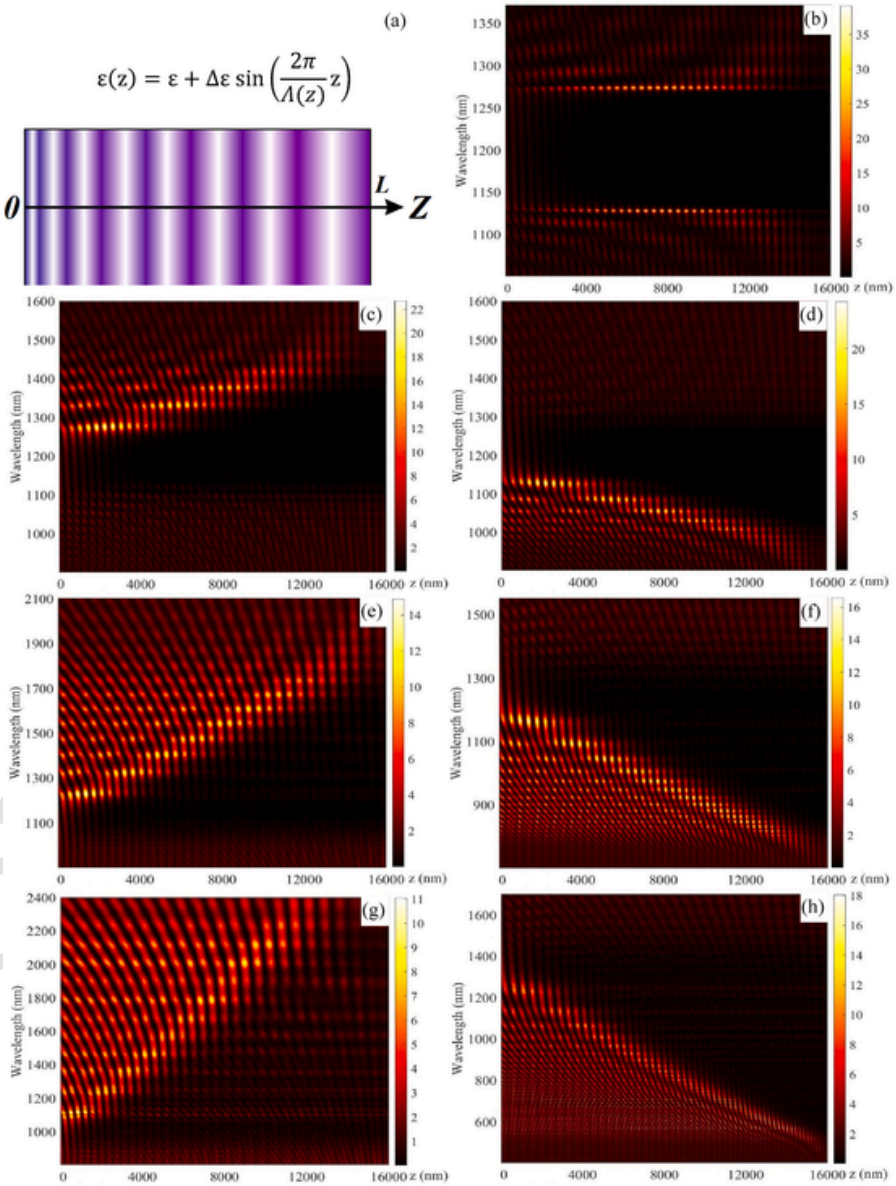


**Fig. 1.** Schematics of the problem: planar rugate PC fragment (a). The evolution of the light intensity inside the PC layer $I(z) = |E_{in}(z)|^2$ when the coordinate $z$ changes in the case of the absence of chirping (b), at contrast of chirping $C = 40$ nm (c,d), at $C = 100$ nm (e,f), and finally at $C = 200$ nm (g,h). Fig. 1(c,e,g) corresponds to the case of positive slope of chirping, and Fig. 1(d,f,h) to the case of negative slope. The parameters of PC layer are: $\varepsilon = 2.25$; $\Delta\varepsilon = 0.5$; $L = 16$ $\mu$m; $\Lambda_{min} = \Lambda - C/2$; $\Lambda_{max} = \Lambda + C/2$; $n_s = 1$. $\Lambda = 400$ nm is the period of modulation in the chirping absence case. The absorption is absent.

$\varepsilon_s = n_s^2$ is the dielectric permittivity of the medium, bordering with the PC layer on both sides. We will consider the linear law of chirping, moreover, both with positive and negative slope, namely, the first case with $\Lambda(z) = az + b = \frac{\Lambda_{\max}-\Lambda_{\min}}{L} z + \Lambda_{\min}$, with $a = \frac{\Lambda_{\max}-\Lambda_{\min}}{L}$, and $b = \Lambda_{\min}$ (chirped PC with positive contrast). In the second case we will have $a = \frac{\Lambda_{\min}-\Lambda_{\max}}{L}$ and $b = \Lambda_{\max}$ (chirped PC with negative contrast). In the first case, along the direction of light propagation, the modulation period increases linearly from the value of $\Lambda_{\min}$ at the input surface to the value of $\Lambda_{\max}$ at the output surface, and in the second case, it decreases linearly from the value of $\Lambda_{\max}$ at the input surface to the value of $\Lambda_{\min}$ at the output surface. The method for solving this problem is described in all details in the paper [45]. This method reduces the problem of the scattering of electromagnetic waves in a one-dimensional inhomogeneous medium to the Cauchy problem for a system of two first-order linear differential equations [45–48]. Here we consider the light normal incidence case only. We will investigate the peculiarities of light localization, specific properties of spectra of reflection, of absorption, of photonic density of states (PDOS) and of density of light energy. The electric field intensities (local intensity [49] in a 1D PC layer are defined as:

$$I_{in}(z) = \left|E_{in}(z)\right|^2, \tag{2}$$

and the absorption coefficients as: $A = 1 - (T + R)$. Here $E_{in}(z)$ is the total electric field inside the PC layer, $T$ and $R$ are the transmission and reflection coefficients, correspondingly. The light energy density in the PC layer will be calculated by the following formula:

$$w = \frac{1}{L}\int_0^L \left|E_{in}(z)\right|^2 dz, \tag{3}$$

and the PDOS by the so-called phase time (or Wigner time) $\tau_\varphi$ which requires only spectral dependence of transmission coefficient $t$ [48]:

$$\begin{aligned}\rho_l &= \frac{\tau_\varphi}{L} \\ &= -\frac{\lambda^2}{2\pi cL}\frac{d}{d\lambda}(\mathrm{Arg}(t)) \\ &= -\frac{\lambda^2}{2\pi cL}\mathrm{Im}\left(\frac{1}{t}\frac{dt}{d\lambda}\right).\end{aligned} \tag{4}$$

The right part of equation (4) can be easily obtained if we consider the derivative part of equation:

$$\begin{aligned}\mathrm{Im}\left(\frac{t'}{t}\right) &= \mathrm{Im}\left(\frac{t_r' + it_i'}{t_r + it_i}\right) \\ &= \mathrm{Im}\left(\frac{t_r' t_r + it_i' t_r - it_r' t_i + t_i' t_i}{t_r^2 + t_i^2}\right) \\ &= \frac{t_i' t_r - t_r' t_i}{t_r^2 + t_i^2} \\ &= \mathrm{Arg}(t)',\end{aligned} \tag{5}$$

where $t' = \frac{dt}{d\lambda}$, and $t_r$ and $t_i$ are real and imaginary parts of $t$.

We will investigate these dependences at different values of contrast of chirping $C = \Lambda_{\max} - \Lambda_{\min}$. First of all, let us note, that as showed in Refs. [33,45] the gradient of the period of modulation has influence on the photonic band gap (PBG) widening, and for PBG boundaries we approximately have $\lambda_1 = 2n_o\Lambda_{\min}$ and $\lambda_2 = 2\left(n_e\Lambda_{\max} + \bar{n}\frac{d\Lambda}{dz}\Delta z\right)$ in the first case of chirping, while for the case of the second type chirping they are approximately defined as: $\lambda_1 = 2\left(n_o\Lambda_{\min} + \bar{n}\frac{d\Lambda}{dz}\Delta z\right)$ and $\lambda_2 = 2n_e\Lambda_{\max}$. Here $n_{o,e} = \sqrt{\varepsilon \pm \frac{\Delta\varepsilon}{2}}$ and $\bar{n} = \frac{n_o+n_e}{2}$.

Fig. 1(a) shows the schematics of the problem: chirped rugate planar PC layer. The rest of figures are the evolution of the light intensity inside the PC layer $I(z) = \left|E_{in}(z)\right|^2$ when the coordinate $z$ changes in the case of the absence of chirping (b), at contrast of chirping $C = 40$ nm (c,d), at $C = 100$ nm (e,f), and finally at $C = 200$ nm (g,h). Fig. 1(c,e,g) corresponds to the case of positive slope of chirping, and Fig. 1(d,f,h) to the case of negative slope.

Fig. 2 shows the spectra of $R$ reflection (curve 1), $A$ absorption (curve 2), $w$ light energy density (curve 3) and of $\rho_l/\rho_{iso}$ relative PDOS (curve 4), again in the case of the absence of chirping (a), at contrast of chirping $C = 40$ nm (b,c), at $C = 100$ nm (d,e), and finally at $C = 200$ nm (f,g). Fig. 2(b,d,f) corresponds to the case of positive slope of chirping, and Fig. 2 (c,e,g) to the case negative slope. $\rho_{iso} = n_s/c$, where $c$ is the speed of light in a vacuum.

As follows from Figs. 1 and 2 in the case of chirping, the widening of PBG takes place and with increase of contrast $C$ this widening increases, too, and the dips in the reflection spectrum appear (Zener tunneling [44,50]). In PCs with continuously changing period due to constructive and destructive interference peaks and dips in the transmission spectrum are possible and the bound modes appear due to Bloch oscillations in chirped crystals and where strong light localization takes place (rainbow trapping) and on these modes one should expect a significant decrease in the lasing threshold. So, in chirped PCs unlike PCs with ideal periodical structure two type of modes are excited, the first ones are modes to the left and right of the PBG (the edge modes) and low-threshold laser generation is also possible on them. The second type of modes are modes inside PBG, these are modes formed due to violation of periodicity of the crystal which are characterized by higher energy localization inside the structure but comparatively low transmission (the bound modes). With a further increase in the chirp contrast, the number of these modes also increases, and they become closely spaced.

Now we pass to investigate the thresholds of laser generation at these bound modes as well as at edge modes. First of all, in this paper we do not take into account nonlinear effects like pump depletion, so the amplification coefficient is uniform and fixed along the entire volume of the structure. We will consider our PC to reach the lasing threshold when the denominator of the transmission coefficient $t$ turns into zero, i.e., the transmission reaches infinity [51]. This condition can be interpreted as when lasing is achieved, one can see a finite outcoming wave in the absence of any incoming wave. So, if the condition $1/t(\lambda, \mathrm{Im}\varepsilon) = 0$ is satisfied for some pair of parameters $(\lambda_{th}, \mathrm{Im}\varepsilon_{th})$, where $\mathrm{Im}\varepsilon<0$ is the amplification, then the lasing is achieved at the wavelength $\lambda_{th}$ with the lasing threshold $\mathrm{Im}\varepsilon_{th}$. It is also worth noting that the lasing can be achieved only at specific wavelengths while at all other wavelengths the lasing is impossible no matter how much the amplification is. Also it's worth noting that in this paper we describe the amplification in terms of imagenary part of dielectric permittivity. Another common way to describe it is to use imaginary part of refractive index but both methods can be used interchangeably:

$$Im(n) = \frac{\left(Re(\varepsilon) + \sqrt{Re(\varepsilon)^2 + Im(\varepsilon)^2}\right)^{\frac{3}{2}} - 2Re(\varepsilon)\sqrt{Re(\varepsilon) + \sqrt{Re(\varepsilon}}}{\sqrt{2}\,Im(\varepsilon)}$$

Fig. 3 shows the values of $\left|\mathrm{Im}(\varepsilon_{th})\right|$ for lasing modes (a) in the case of the absence of chirping, and (b,c) at contrast of chirping $C = 200$ nm. Fig. 3(b) corresponds to the case of positive slope of chirping, and Fig. 3 (c) to the case of negative slope. In Fig. 3(a) we can clearly see the decrease in the lasing threshold of laser modes near the boundaries of the PBG, while inside the PBG itself laser generation is not observed at all. However, Fig. (b)–(c) are much more complex with a non-monotonic dependence of the threshold on wavelength, which is also related to the

CORRECTED PROOF

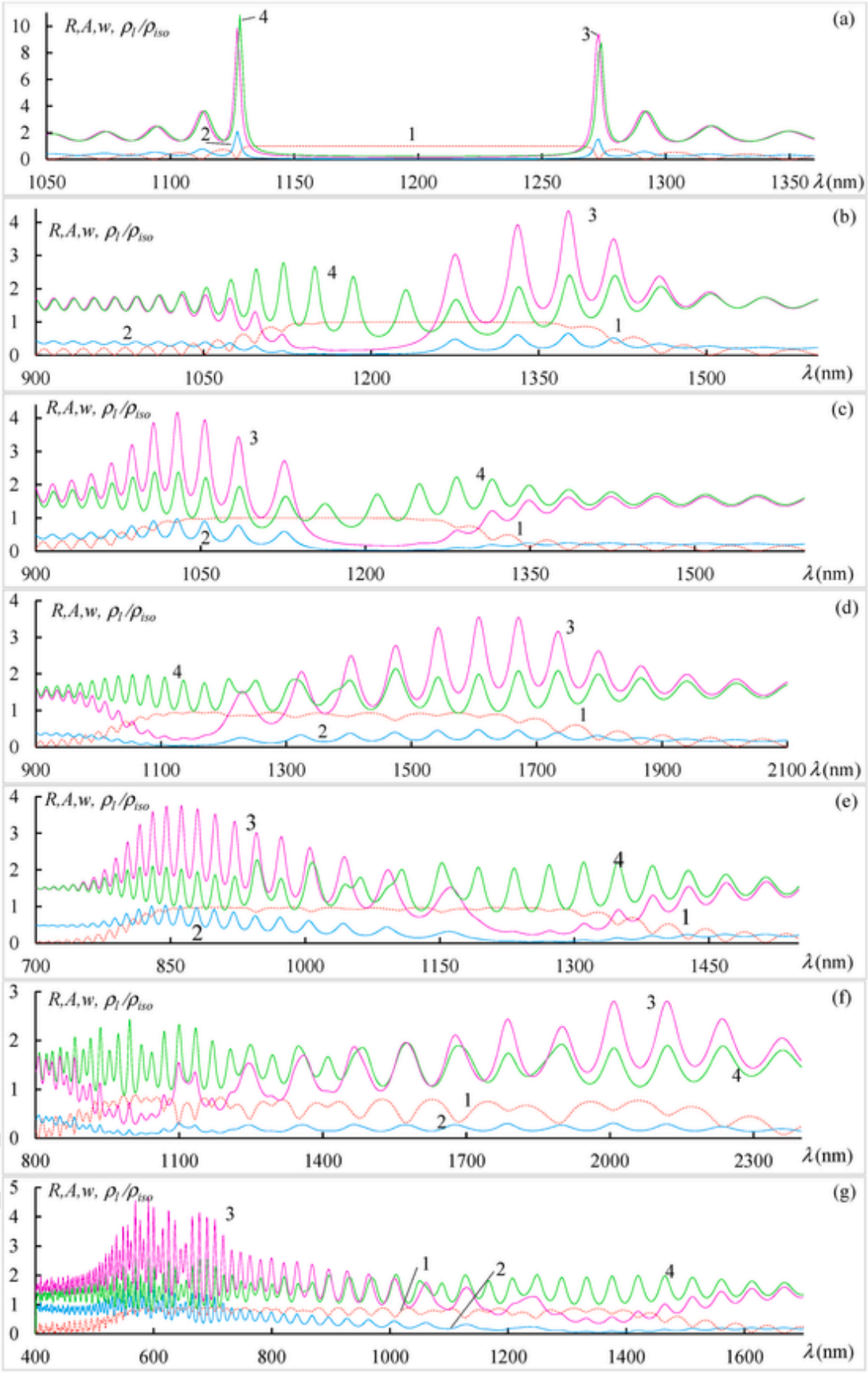
(a)
R,A,w, ρl/ρiso
λ(nm)
(b)
(c)
(d)
(e)
(f)
(g)

**Fig. 2.** The spectra of $R$ reflection (curve 1), $A$ absorption (curve 2), $w$ light energy density (curve 3) and of $\rho_l/\rho_{iso}$ relative PDOS (curve 4), again in the case of the absence of chirping (a), at contrast of chirping $C = 40$ nm (b,c), at $C = 100$ nm (d,e), and finally at $C = 200$ nm (f,g). Fig. 2(b,d,f) corresponds to the case of positive slope of chirping, and Fig. 2(c,e,g) to the case negative slope. The absorption is homogeneous and $\mathrm{Im}(\varepsilon) = 10^{-3}$. The other parameters are the same as in Fig.1.

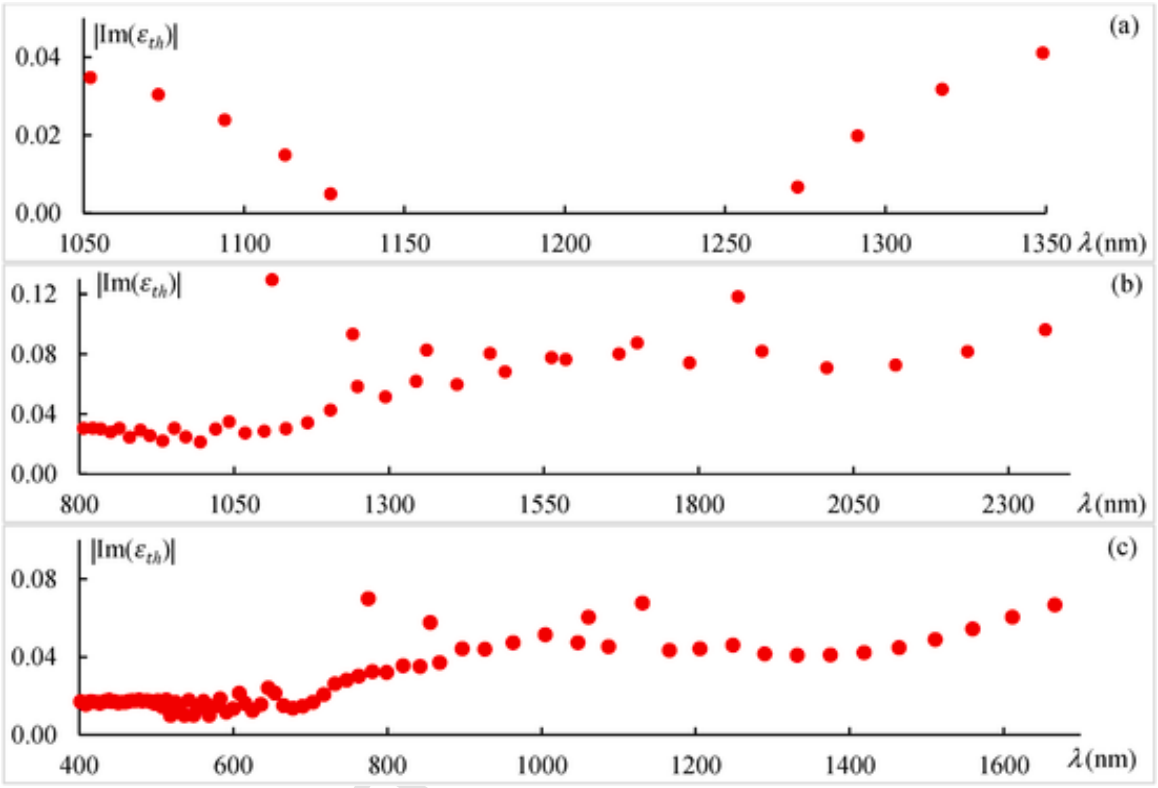


**Fig. 3.** The values of $\left|\mathrm{Im}\left(\varepsilon_{th}\right)\right|$ for lasing modes (a) in the case of the absence of chirping, and (b,c) at contrast of chirping $C = 200$ nm. Fig. 3(b) corresponds to the case of positive slope of chirping, and Fig. 3(c) to the case of negative slope. The other parameters are the same as in Fig.1.

complex spectra of the reflection and transmission. This fact might also explain that at some wavelengths a significantly higher threshold is observed. In addition, as can be seen from Fig. 3(c) at value $|\mathrm{Im}(\varepsilon)| = 0.02$ simultaneous laser generation in all, closely spaced modes in all visible region of the spectrum, is possible. Then, as can be seen in Fig. 3(b and c) at $|\mathrm{Im}(\varepsilon)| = 0.08$ simultaneous laser generation in all modes in the spectral region from 400 nm to 2400 nm is possible, moreover both in forward and backward directions.

Thus, the creation of closely spaced, multi-mode, broadband and low-threshold lasers based on resonators in the form of chirped rugate PCs is quite possible.

And now, to generalize our results, we will consider a chirped but stratified PCs. We will consider a binary PC (Fig. 4(a)) with dielectric permittivities of layers $\mathrm{Re}\left(\varepsilon_1\right) = 1.85$ and $\mathrm{Re}\left(\varepsilon_2\right) = 2.65$. The quarter-wave criterion for layer thicknesses is fulfilled, that is:

$$h_{1j} = \Lambda_j \frac{n_2}{n_1 + n_2}, h_{2j} = \Lambda_j \frac{n_1}{n_1 + n_2}. \tag{7}$$

Here $j$ is the ordinal number of the cell, $n_1 = \sqrt{\varepsilon_1}$ and $n_2 = \sqrt{\varepsilon_2}$. The period $\Lambda_j$ is found by the formula $\Lambda(z) = \left(280 + 500\frac{z}{L}\right)$ for stratified chirped PC with positive contrast of chirping and $\Lambda(z) = \left(540 - 350\frac{z}{L}\right)$ for negative contrast of chirping, here $L = 16$ μm, as the thickness of above considered rugate PC, while the actual thickness of the stratified PC is $d \lesssim L$. The period for each cell is calculated at its left boundary (e.g. $\Lambda_1 = \Lambda(0)$, $\Lambda_2 = \Lambda(\Lambda_1)$, $\Lambda_3 = \Lambda(\Lambda_1 + \Lambda_2)$ etc.). We keep adding new cells as long as the condition $d = \sum_j^N \Lambda_j \le L$ is satisfied. The largest $N$ that satisfies this condition is the number of cells of our stratified PC with thickness $L$. As above we assume that stratified PC is being in vacuum, that is $n_s = 1$, and the light normal incidence case we will consider.

Fig. 4 b,c shows the spectra of $R$ reflection (curve 1), $A$ absorption (curve 2), $w$ light energy density (curve 3) and of $\rho_l/\rho_{iso}$ relative PDOS (curve 4) for chirped stratified PC with positive contrast of chirping (b), and with negative contrast of chirping (c).

And now we pass to investigate the thresholds of laser generation for this PC.

Comparison of the results in Figs. 2 and 3 for the chirped rugate PCs with similar results in Figs. 4 and 5 for the chirped stratified PCs shows, that the main conclusion presented above for the chirped rugate PCs that the creation of closely spaced, multi-mode, broadband and low-threshold lasers based on resonators in the form of chirped rugate PCs is quite possible, also takes place for the chirped stratified PCs too.

In conclusion of this paragraph, we, for comparison, in Figs. 6 and 7 have presented similar dependences for the Fabry-Perot laser resonator with parameters: $\mathrm{Re}(\varepsilon) = 2.196$, $L = 16$ μm, power reflection coefficient of the mirrors $R_1 = R_2 = 0.109$. Let us note that our results for the Fabry-Perot resonator agree with similar results in Ref. [52]. Note that Ref. [52] presents threshold values for the imaginary part of the wave vector, while we present threshold values for the imaginary part of the permittivity. At the same time, comparison of the results for the Fabry-

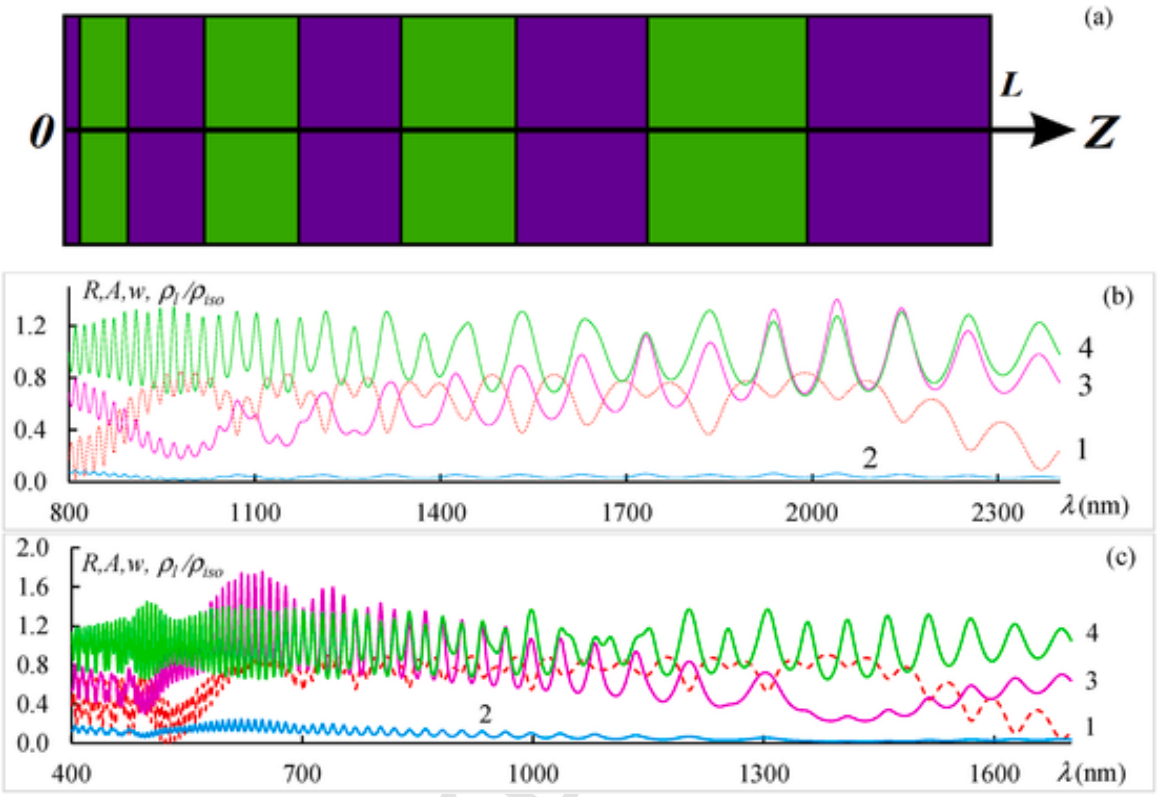


**Fig. 4.** Schematics of the problem: planar chirped stratified PC fragment (a). The spectra of $R$ reflection (curve 1), $A$ absorption (curve 2), $w$ light energy density (curve 3) and of $\rho_l/\rho_{iso}$ relative PDOS (curve 4) for chirped stratified PC with positive contrast of chirping (b), and negative contrast of chirping (c). $\mathrm{Im}\,(\varepsilon_1) = \mathrm{Im}\,(\varepsilon_2) = 10^{-3}$.

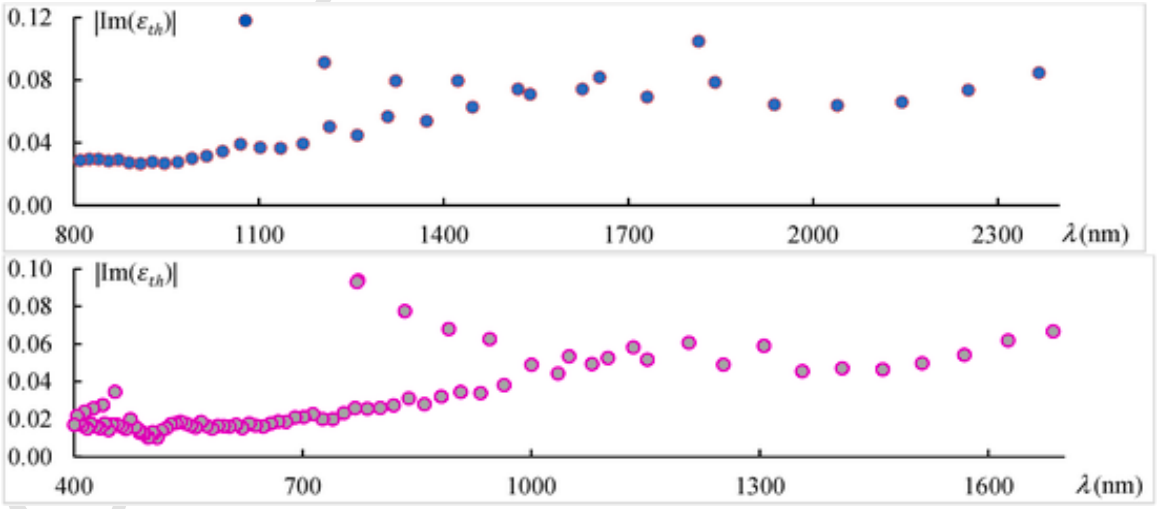


**Fig. 5.** The values of $\left|\mathrm{Im}\,(\varepsilon_{th})\right|$ for lasing modes in the case of stratified chirped PC (a) with the positive contrast of chirping and (b) with the negative contrast of chirping.

Perot resonator with similar results for PCs with an ideal periodic structure and for chirped PCs demonstrates their significantly different characters. It is worth noting that despite the fact that a laser based on a Fabry-Perot resonator is much easier to realize in practice, a laser based on a chirped PC has one important advantage, namely, the possibility of fine-tuning the reflection and transmission spectra and, consequently, controlling the spectrum of lasing thresholds. This advantage makes it possible to control the emission spectrum by changing the chirping parameters, which is important for a white laser, since the "quality" of white light depends on the ratio of red, green, and blue color intensities in the spectrum. In the case of a Fabry-Perot resonator,

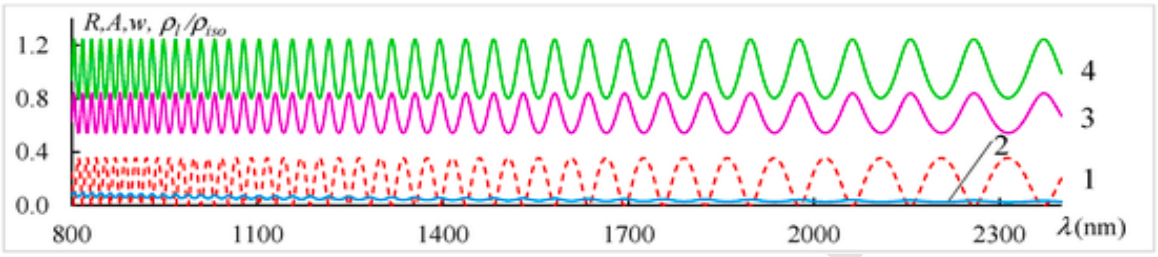


**Fig. 6.** The spectra of $R$ reflection (curve 1), $A$ absorption (curve 2), $w$ light energy density (curve 3) and of $\rho_l/\rho_{iso}$ relative PDOS (curve 3) for the laser resonator Fabry-Perot.

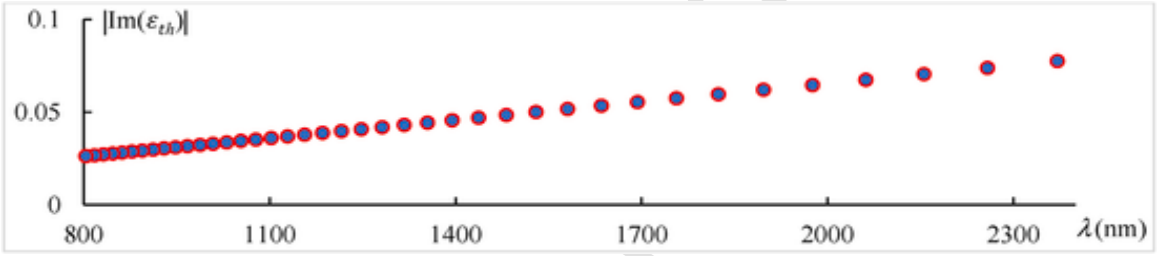


**Fig. 7.** The values of $\left|\mathrm{Im}\left(\varepsilon_{th}\right)\right|$ for lasing modes for the laser resonator Fabry-Perot.

all modes of the resonator change equally when the resonator parameters are changed.

And now, let us consider the question on how do we propose to realize this resonator? As have well known 1D PCs can be created by modulation of the medium parameters in external periodic inhomogeneous fields. In particular, photopolymers are of great interest since they change their properties when exposed to light, often in the ultraviolet or visible parts of the electromagnetic spectrum [53]. Of course, in this way one can create chirped rugate PCs. The plasma enhanced chemical vapor deposition technology [54] is another way which makes it possible to obtain chirped continuous PCs with high optical contrast, but it is a rather complicated and expensive process [55].

After creating chirped rugate PC we can make it active by enriching with dye molecules. To get a broadband emission line, we can, as in Ref. [55], use dye molecules of PVA/SB420, PVA + LC/CM540 and PVA + LC/DCM, or as in Refs. [56–59] use a rare-earth metal ions ($Eu^{2+}$, $Ce^{3+}$) placed in matrices ($CaAlSiN_3$, $Lu_3Al_5O_{12}$, $(La,Y)_3Si_6N_{11}$). Using different methods, it is possible to obtain both harmonic chirped PCs and stratified chirped active PCs. In particular, the paper [60] shows an example of a self-assembled nanoparticle-based distributed feedback (DFB) laser based on a hybrid organic dye-doped inorganic nanoparticle 1D PC architecture, the papers [61,62] show a way to create a one-dimensional dielectric resonator doped with $Er^{3+}$ in different geometrical configurations, and [63] also considers the case of doping a one-dimensional photonic crystal with rare earth metals such as $Eu^{3+}$ to obtain properties where light confinement causes an improvement in optical and/or spectroscopic properties. In Ref. [64] the authors have described the first example of a self-assembled nanoparticle-based DFB laser based on a hybrid organic dye doped inorganic nanoparticle 1D PC architecture. This system displays stimulated emission at the blue edge of the PBG, thus suggesting that the peak wavelength of the laser can be tuned by simply varying the position of the photonic band edge.

In our opinion, such systems could be the basis for obtaining multimode low-threshold lasers. Of course, in a real experimental implementation of such lasers there might be numerous new problems.

## 3. Conclusions

In conclusion, we theoretically investigated the possible simultaneous laser generation in all, closely spaced modes of chirped both rugate and stratified PCs in the entire visible region of the spectrum. The spectra of reflection, field localization as well as relative PDOS and absorption for both rugate and stratified PCs, as well as Fabry-Perot resonator are computed and compared, for PCs with different chirping constants, as well as in strictly periodic PCs. It was shown that there are two kinds of modes in chirped PCs: edge modes and bound modes. We also calculated the threshold values for mentioned structures. In addition, we note that with the ability to control the chirp contrast, it becomes possible to obtain a white laser with a simple system on a chip, which can find wide application ranging from miniaturized coherent light source, optical sensing, to visible light communication. It should be noted that in this paper we considered the general case and did not take into account the refractive index dispersion of the constituent materials, which can have a significant effect on the lasing when considering a wide spectral range. In addition, the results in this paper were obtained without considering nonlinear effects like pump depletion. In the next work we plan to add them by employing rate equations.

## Uncited references

[49].

## CRediT authorship contribution statement

**A.H. Gevorgyan:** Conceptualization, Formal analysis, Funding acquisition, Investigation, Methodology, Project administration, Supervision, Writing – original draft, Writing – review & editing. **N.A. Vanyushkin:** Formal analysis, Investigation, Methodology, Resources, Software, Validation, Visualization, Writing – original draft, Writing – review & editing. **I.M. Efimov:** Data curation, Formal analysis, Investigation, Resources, Software, Validation, Writing – original draft, Writing – review & editing.

## Declaration of competing interest

The authors declare that they have no known competing financial interests or personal relationships that could have appeared to influence the work reported in this paper.

## Data availability

No data was used for the research described in the article.

## Acknowledgment

The work was supported by the Russian Science Foundation (Grant № 24-22-00283).

## References

[1] N. Davidson, S. Mahler, A. Friesem, Andrew Forbes, Complex-light lasers, Opt Photon. News 33 (2022) 26–33, https://doi.org/10.1364/OPN.33.5.000026.
[2] A. Forbes, Structured light: tailored for purpose, Opt Photon. News 31 (2020) 24–31, https://doi.org/10.1364/OPN.31.6.000024.
[3] F. Qian, Y. Li, S. Gradečak, H.-G. Park, Y. Dong, Y. Ding, Z.L. Wang, C.M. Lieber, Multi-quantum-well nanowire heterostructures for wavelength controlled lasers, Nature 7 (2008) 701–706.
[4] X.P. Hu, G. Zhao, Z. Yan, X. Wang, Z.D. Gao, H. Liu, J.L. He, S.N. Zhu, High-power red-green-blue laser light source based on intermittent oscillating dual-wavelength Nd:YAG laser with a cascaded $LiTaO_3$ superlattice, Opt. Lett. 33 (2008) 408–410.
[5] S.K.Y. Tang, Z. Li, A.R. Abate, J.J. Agresti, D.A. Weitz, D. Psaltis, G.M. Whitesides, A multi-color fast-switching microfluidic droplet dye laser, Lab Chip 9 (2009) 2767–2771.
[6] Y. Ding, Q. Yang, X. Guo, S. Wang, F. Gu, J. Fu, Q. Wan, J. Cheng, L. Tong, Nanowires/microfibre hybrid structure multicolor laser, Opt Express 17 (2009) 21813–21818.
[7] K. Yamashita, N. Takeuchi, K. Oe, H. Yanagi, Simultaneous RGB lasing from a single-chip polymer device, Opt. Lett. 35 (2010) 2451–2453.
[8] C. Dang, J. Lee, C. Breen, J.S. Steckel, S. Coe-Sullivan, A. Nurmikko, Red, green and blue lasing enabled by single-exciton gain in colloidal quantum dot films, Nat. Nanotechnol. 7 (2012) 335–339.
[9] J.J. Wierer, J.Y. Tsao, D.S. Sizov, Comparison between blue lasers and light-emitting diodes for future solid-state lighting, Laser Photon. Rev. 7 (2013) 963.
[10] S. Chen, X. Zhao, Y. Wang, J. Shi, D. Liu, White light emission with red-green-blue lasing action in a disordered system of nanoparticles, Appl. Phys. Lett. 101 (2012) 123508.
[11] A. Neumann, J.J. Wierer, W. Davis, Y. Ohno, S.R. Brueck, J.Y. Tsao, Four-color laser white illuminant demonstrating high color-rendering quality, Opt Express 19 (2011) A982–A990.
[12] F. Fan, S. Turkdogan, Z. Liu, D. Shelhammer, C.Z. Ning, A monolithic white laser, Nat. Nanotechnol. 10 (2015) 796.
[13] L. Jin, Z. Liu, Y. Zhang, Y. Wu, Y. Liu, H. Deng, Q. Song, S. Xiao, Lanthanide-doped nanocrystals in high-Q microtoroids for stable on-chip white-light lasers, Photon. Res. 10 (2022) 1594–1601.
[14] A. Adamow, A. Szukalski, L. Sznitko, et al., Electrically controlled white laser emission through liquid crystal/polymer multiphases, Light Sci. Appl. 9 (2020) 19.
[15] B. Chen, L. Hong, C. Hu, Z. Li, White laser realized via synergic second-and third-order nonlinearities, Research (2021) 2021.
[16] A. Adamow, A. Szukalski, A. Justyniarski, L. Sznitko, J. Mysliwiec, Light amplification in tunable multicolor liquid crystalline system, J. Lumin. 220 (2020) 116903.
[17] X.P. Hu, G. Zhao, Z. Yan, X. Wang, Z.D. Gao, H. Liu, J.L. He, S.N. Zhu, High-power red-green-blue laser light source based on intermittent oscillating dual-wavelength Nd:YAG laser with a cascaded LiTaO3LiTaO3 superlattice, Opt. Lett. 33 (2008) 408–410.
[18] D. Huang, Y. Xie, D. Lu, Z. Wang, J. Wang, H. Yu, H. Zhang, Demonstration of a white laser with V2C MXene-based quantum dots, Adv. Mater. 31 (2019) 1901117.
[19] C.M. Rushworth, et al., On-chip cavity-enhanced absorption spectroscopy using a white light-emitting diode and polymer mirrors, Lab Chip 15 (2015) 711–717.
[20] A. Kotani, et al., EndoV/DNA ligase mutation scanning assay using microchip capillary electrophoresis and dual-color laser-induced fluorescence detection, Anal. Methods 4 (2012) 58–64.
[21] G. Cossu, et al., 3.4 Gbit/s visible optical wireless transmission based on RGB LED, Opt Express 20 (2012) B501–B506.
[22] J.J. Wierer Jr, J.Y. Tsao, D.S. Sizov, Comparison between blue lasers and light-emitting diodes for future solid-state lighting, Laser Photon. Rev. 7 (2013) 963–993.
[23] X.M. Li, et al., CsPbX3 quantum dots for lighting and displays: room temperature synthesis, photoluminescence superiorities, underlying origins and white light-emitting diodes, Adv. Funct. Mater. 26 (2016) 2435–2445.
[24] L. Jin, X. Chen, Y. Wu, X. Ai, X. Yang, S. Xiao, Q. Song, Dual-wavelength switchable single-mode lasing from a lanthanide-doped resonator, Nat. Commun. 13 (2022) 1727.
[25] B.-S. Moon, T.K. Lee, W.C. Jeon, S.K. Kwak, Y.-J. Kim, D.-H. Kim, Continuous-wave upconversion lasing with a sub-10 W cm−2 threshold enabled by atomic disorder in the host matrix, Nat. Commun. 12 (2021) 4437.
[26] H. Xin, Y. Li, Y.-C. Liu, Y. Zhang, Y.-F. Xiao, B. Li, Optical forces: from fundamental to biological applications, Adv. Mater. 32 (2020) 2001994.
[27] Y. Hu, L. Shao, S. Arnold, Y.-C. Liu, C.-Y. Ma, Y.-F. Xiao, Mode broadening induced by nanoparticles in an optical whispering-gallery microcavity, Phys. Rev. A 90 (2014) 043847.
[28] C. Zhang, C.-L. Zou, Y. Zhao, C.-H. Dong, C. Wei, H. Wang, Y. Liu, G.-C. Guo, J. Yao, Y.S. Zhao, Organic printed photonics: from microring lasers to integrated circuits, Sci. Adv. 1 (2015) e1500257.
[29] C. Huang, C. Zhang, S. Xiao, Y. Wang, Y. Fan, Y. Liu, N. Zhang, G. Qu, H. Ji, J. Han, Ultrafast control of vortex microlasers, Science 367 (2020) 1018–1021.
[30] X.-R. Mao, Z.-K. Shao, H.-Y. Luan, S.-L. Wang, R.-M. Ma, Magic angle lasers in nanostructured moiré superlattice, Nat. Nanotechnol. 16 (2021) 1099–1105.
[31] L. Jin, Z. Liu, Y. Zhang, Y. Wu, Y. Liu, H. Deng, Q. Song, S. Xiao, A highly-efficient single segment white random laser, ACS Nano 12 (2018) 11847–11859.
[32] X. Shi, Y. Bian, J. Tong, D. Liu, J. Zhou, Z. Wang, Chromaticity-tunable white random lasing based on a microfluidic channel, Opt Express 28 (2020) 13576.
[33] D.M. Sedrakian, A.H. Gevorgyan, A.Zh Khachatrian, V.D. Badalian, Photonic Band Gap in 1D Photonic Crystals with gradient profile of pitch and amplitude of modulation, Opt Commun. 271 (2007) 451–456, https://doi.org/10.1016/j.optcom.2006.10.068.
[34] D.S. García, D. Cardador, D. Vega, M. Santos, F. Dios, A. Rodriguez, Bandgap widening in macroporous silicon photonic crystals by multiperiodic structures, J. Phys. Commun. 2 (2018) 055014, https://doi.org/10.1088/2399-6528/aac0ec.
[35] S. Sharma, A. Mondal, R. Das, Geometric representation of adiabatic distributed-Bragg-reflectors and broadening the photonic bandgap, Opt Express 29 (2021) 43303–43315, https://doi.org/10.1364/OE.446783.
[36] K.L. Tsakmakidis, A.D. Boardman, O. Hess, 'Trapped rainbow' storage of light in metamaterials, Nature 450 (2007) 397–401, https://doi.org/10.1038/nature06285.
[37] L. Chen, G.P. Wang, Q. Gan, F.J. Bartoli, Trapping of surface-plasmon polaritons in a graded Bragg structure: frequency-dependent spatially separated localization of the visible spectrum modes, Phys. Rev. B 80 (R) (2009) 161106, https://doi.org/10.1103/PhysRevB.80.161106.
[38] Y. Shen, J. Fu, G. Yu, Rainbow trapping in one-dimensional chirped photonic crystals composed of alternating dielectric slabs, Phys. Lett. 375 (2011) 3801–3803, https://doi.org/10.1016/j.physleta.2011.08.023.
[39] S. Sharma, A. Mondal, R. Das, Infrared rainbow trapping via optical Tamm modes in an one-dimensional dielectric chirped photonic crystals, Opt Lett. 46 (2021) 4566–4569, https://doi.org/10.1364/OL.437958.
[40] Z. Hayran, H. Kurt, K. Staliunas, Rainbow trapping in a chirped three-dimensional photonic crystal, Sci. Rep. 7 (2017) 3046, https://doi.org/10.1038/s41598-017-03454-w.
[41] J. Xu, S. Xiao, P. He, Y. Wang, Y. Shen, L. Hong, Y. Luo, B. He, Slow wave and truly rainbow trapping in a one-way terahertz waveguide, Opt Express 29 (7) (2021) 11328–11341, https://doi.org/10.1364/OE.447874.
[42] S. Elshahat, C. Lu, Bidirectional rainbow trapping in 1-D chirped topological photonic crystal, Front. Physiol. 10 (2022) 831203, https://doi.org/10.3389/fphy.2022.831203.
[43] C.Q. Cook, A. Amir, Theory of chirped photonic crystals in biological broadband reflectors, Optica 3 (2016) 1436–1439, https://doi.org/10.1364/OPTICA.3.001436.
[44] M. Bellingeri, A. Chiasera, I. Kriegel, F. Scotognella, Optical properties of periodic, quasi-periodic, and disordered one dimensional photonic structures, Opt. Mater. 72 (2017) 403–421, https://doi.org/10.1016/j.optmat.2017.06.033.
[45] A.H. Gevorgyan, N.A. Vanyushkin, M.S. Rafayelyan, Light localization in 1D chirped photonic crystals, Eur. Phys. J. Plus 137 (2022) 719.
[46] D.M. Sedrakian, A.H. Gevorgyan, A.Zh Khachatrian, Reflection of a plane electromagnetic wave oblique incident onto a one-dimensional isotropic dielectric medium with an arbitrary refractive index, Opt Commun. 192 (2001) 135–143, https://doi.org/10.1016/S0030-4018(01)01201-9.
[47] N.A. Vanyushkin, A.H. Gevorgyan, S.S. Golik, Scattering of a plane wave by an inhomogeneous 1D dielectric layer with gradient refractive index, Opt. Mater. 127 (2022) 112306, https://doi.org/10.1016/j.optmat.2022.112306.
[48] N.A. Vanyushkin, A.H. Gevorgyan, And again, about lasing threshold, light localization, and density of states in 1D photonic crystals, Photon. Nanostruct: Fundam. Appl. 54 (2023) 101134, https://doi.org/10.1016/j.photonics.2023.101134.
[49] I.S. Fogel, J.M. Bendickson, M.D. Tocci, M.J. Bloemer, M.l. Scalora, C.M. Bowden, J.P. Dowling, Spontaneous emission and nonlinear effects in photonic bandgap materials, Pure Appl. Opt. 7 (1998) 393–407.
[50] R. Sapienza, P. Costantino, D. Wiersma, M. Ghulinyan, C.J. Oton, L. Pavesi, Optical analogue of electronic Bloch oscillations, Phys. Rev. Lett. 91 (2003) 263902.
[51] A. Yariv, P. Yeh, Optical Waves in Crystals, Wiley, New York, 1984.
[52] L.M. Blinov, Density of states and lasing threshold in dye-doped cholesteric liquid crystals, J. Nonlinear Opt. Phys. Mater. 19 (2010) 15–32, https://doi.org/10.1142/S0218863510005078.
[53] M. Campbell, D.N. Sharp, M.T. Harrison, R.G. Denning, A.J. Turberfield, Fabrication of photonic crystals for the visible spectrum by holographic lithography, Nature 404 (6773) (2000) 53–56, https://doi.org/10.1038/35003523.
[54] S. Lim, J.H. Ryu, J.F. Wager, T.K. Plant, Rugate filters grown by plasma-enhanced chemical vapor deposition, Thin Solid Films 245 (1–2) (1994) 141–145,

CORRECTED PROOF

https://doi.org/10.1016/0040-6090(94)90889-3.
[55] R. Paschotta, Encyclopedia of Laser Physics and Technology, Wiley-VCH, Berlin, 2008.
[56] H. Wu, Z. Hao, G.-H. Pan, L. Zhang, H. Wu, X. Zhang, L. Zhang, J. Zhang, Phosphor-SiO2 composite films suitable for white laser lighting with excellent color rendering, J. Eur. Ceram. Soc. 40 (2020) 2439–2444, https://doi.org/10.1016/j.jeurceramsoc.2020.01.020.
[57] Y. Mou, Q. Wang, Z. Guo, J. Zhao, Z. Yu, Y. Peng, Nitride phosphor-in-glass films enabling high-performance white light in transmissive and reflective laser lighting, Ceram. Int. 49 (2023) 11821–11828, https://doi.org/10.1016/j.ceramint.2022.12.028.
[58] T. Deng, L. Huang, S. Li, Q. Zhu, L. Wang, T. Takeda, N. Hirosaki, R.-J. Xie, Thermally robust orange-red-emitting color converters for laser-driven warm white light with high overall optical properties, Laser Photon. Rev. 16 (2022) 2100722, https://doi.org/10.1002/lpor.202100722.
[59] X. Peng, S. Li, B. Zhang, et al., Orange-emitting MgO–(Sr,Ba)3SiO5:Eu composite phosphor ceramics for turn signals and warm white laser lighting, J. Am. Ceram. Soc. 106 (2023) 1945–1953, https://doi.org/10.1111/jace.18900.
[60] F. Scotognella, Multilayer plasmonic photonic structures embedding photochromic molecules or optical gain molecules, Physica E Low Dimens. Syst. Nanostruct. 120 (2020) 114081, https://doi.org/10.1016/j.physe.2020.114081.
[61] A. Chiasera, et al., Coherent emission from fully Er3+ doped monolithic 1-D dielectric microcavity fabricated by rf-sputtering, Opt. Mater. 87 (2019) 107–111, https://doi.org/10.1016/j.optmat.2018.04.057.
[62] C. Meroni, F. Scotognella, Y. Boucher, et al., Low-threshold coherent emission at 1.5 μm from fully $Er^{3+}$ doped monolithic 1D dielectric microcavity fabricated using radio frequency sputtering, Ceramics 2 (2019) 74–85, https://doi.org/10.3390/ceramics2010007.
[63] L. Zampedri, et al., Spectroscopic assessment of rare-earth activated planar waveguides and microcavities, Appl. Surf. Sci. 248 (2005) 3–7, https://doi.org/10.1016/j.apsusc.2005.03.022.
[64] F. Scotognella, D.P. Puzzo, A. Monguzzi, et al., Nanoparticle one-dimensional photonic-crystal dye laser, Small 5 (18) (2009) 2048–2052, https://doi.org/10.1002/smll.200900331.

CORRECTED PROOF



View publication stats